J. Membrane Biol. 188, 213–226 (2002)
DOI: 10.1007/s00232-001-0185-z

The Journal of
Membrane
Biology

Blue Light Modulation of Ion Transport in the *slime* Mutant of *Neurospora crassa*

N.N. Levina[1], A.Y. Dunina-Barkovskaya[2], S. Shabala[3], R.R. Lew[1]
[1]Biology Department, York University, 4700 Keele St., Toronto, Ontario, M3J 1P3, Canada
[2]A.N. Belozersky Institute, Moscow State University, Moscow, Russia
[3]School of Agricultural Sciences, University of Tasmania, Hobart, Australia

Received: 28 December 2001/Revised: 16 April 2002

Abstract. Blue light is the primary entrainment signal for a number of developmental and morphological processes in the lower eucaryote *Neurospora crassa*. Blue light regulates photoactivation of carotenoid synthesis, conidiation, phototropism of perithecia and circadian rhythms. Changes in the electrical properties of the plasma membrane are one of the fastest responses to blue light irradiation. To enable patch-clamp studies on light-induced ion channel activity, the wall-less *slime* mutant was used. Patch-clamp experiments were complemented by non-invasive ion-selective measurements of light-induced ion fluxes of *slime* cells using the vibrating probe technique. Blue light usually caused a decrease in conductance within 2–5 minutes at both negative and positive voltages, and a negative shift in the reversal potential in whole-cell patch-clamp measurements. Both K^+ and Cl^- channels contribute to the inward and outward currents, based on the effects of TEA (10 mM) and DIDS (500 μM). However, the negative shift in the reversal potential indicates that under blue light the Cl^- conductance becomes dominant in the electrical properties of the *slime* cells due to a decrease of K^+ conductance. The ion-selective probe revealed that blue light induced the following changes in the net ion fluxes within 5 minutes: 1) decrease in H^+ influx; 2) increase in K^+ efflux; and 3) increase in Cl^- influx. Ca^{2+} flux was unchanged. Therefore, blue light regulates an ensemble of transport processes: H^+, Cl^-, and K^+ transport.

Key words: *Slime* — Blue light — Patch clamp — Ion flux — K^+ channels — Cl^- channels

Correspondence to: R.R. Lew; email: planters@yorku.ca

Introduction

Blue light (BL) regulates many aspects of fungal and plant development, and circadian rhythms. In comparison to plants with their complexity of photobiological reactions and the diversity in BL photoreceptors, the fungus *Neurospora crassa* is a simpler, but genetically well-characterized model organism appropriate for studying mechanisms of BL reception and control of photomorphogenesis.

Some photoreceptors of BL have been identified and cloned from *Arabidopsis thaliana* (Ahmad & Cashmore, 1993; Ahmad et al., 1998b; Cashmore et al., 1999; Briggs et al., 2001). Flavin- and pterin-binding photolyase homologues, cryptochrome 1 (CRY1), and cryptochrome 2 (CRY2) (Ahmad & Cashmore, 1993, 1996; Ahmad et al., 1998a; Bagnall, King & Hangarter, 1996; Lin et al., 1995), and a flavin-containing protein kinase, phototropin (NPH1) (Christie et al., 1998; Huala et al., 1997), have been identified as BL photoreceptors involved in the BL-regulated hypocotyl growth, entrainment of the circadian clock and phototropism, respectively. NPH1 was shown to be associated with plasma membrane (Reymond et al., 1992; Huala et al., 1997). For *Vicia faba* stomatal guard cells, in which BL regulates turgor pressure, it was demonstrated that BL is sensed by a chloroplastic carotenoid photoreceptor, zeaxanthin (Frechilla et al., 1999). In spite of accumulated data on the nature of chromophores, the mechanism of the signal-transduction cascade downstream of photoreceptors is poorly understood.

Changes in plasma membrane electrical properties are the fastest responses to blue light, implicating the involvement of plasma membrane ion transporters in the BL signaling network. Hyperpolarization of the plasma membrane due to activation of the plasma membrane proton pump in *Vicia faba* guard cells can be detected as early as 30 sec after the illumination

(Assmann, Simoncini & Schroeder, 1985; Kinoshita & Shimazaki, 1999); depolarization of the plasma membrane and activation of anion channels in *Arabidopsis* seedlings begin within seconds of BL illumination (Cho & Spalding, 1996; Noh & Spalding, 1998), and activation of K^+ channels in flexor cells from *Samanea saman* was observed after 20 sec of BL illumination (Suh, Moran & Lee, 2000).

In *Neurospora crassa*, blue light regulates several developmental and morphological processes (reviewed by Linden et al., 1999). Two key components in the blue light signal-transduction pathway in *N. crassa,* the '*white collar*' WC1 and WC2 regulatory proteins, have been identified. WC1 and WC2 are putative transcriptional factors regulating the expression of blue light-induced genes (Ballario et al., 1996; Linden, Ballario & Macino, 1997; Talora et al., 1999). These proteins are two central components of blue light signal transduction, since *wc-1* and *wc-2* mutants are completely insensitive to light: they do not demonstrate any of the early or late light responses (Harding & Turner, 1981; Degli-Innocenti & Russo, 1984; Lauter, Yamashiro & Yanofsky, 1997). Both WC proteins are considered to function in transcriptional gene regulation after BL illumination. In addition, the WC genes have repeats with homology to PAS domains found in some sensory proteins, which suggests that WC1 and WC2 may be photoreceptors in *N. crassa*, and, therefore, represent a unique class of molecules able to operate in both signal perception and transcriptional control (Ballario & Macino, 1997). Although WC proteins are not localized exclusively in membrane fractions (Schwerdtfeger & Linden, 2000), their functional connection with plasma membrane transport systems is possible, since photoinduced electrical changes are not observed in *wc-1* mutant (Levina et al., 1988). In wild type, an increase in the plasma membrane input resistance followed by hyperpolarization was recorded as early as 2–5 min after illumination of the hyphae (Potapova et al., 1984). The possibility that changes in ion transport across the plasma membrane are directly associated with BL photoreception and subsequent signal transduction is supported by findings that the *N. crassa* genome contains sequences with high homology to the plasma membrane-associated *Arabidopsis* photoreceptor NPH1 (BLAST search) (Neurospora Sequencing Project. Whitehead Institute/MIT Center for Genome Research [www.genome.wi.mit.edu]).

We used the patch-clamp technique to analyze the changes in ion transport, which occur during blue light signal transduction in *N. crassa*. The use of patch clamp in fungi is difficult because of the presence of cell wall on the surface of fungal cells. Two methods for cell wall removal to allow access to the plasma membrane have been used. One is the enzymatic removal of cell wall material in patch-clamp measurements reported for *Uromyces appendiculatus* (Zhou et al., 1991), *Saprolegnia ferax* (Garrill et al., 1993), yeast (Bertl & Slayman, 1992; Gustin et al., 1986; Watts et al., 1998) and *N. crassa* (Levina et al., 1995). Another approach is to plasmolyze the cell, and then use laser ablation of the cell wall, permitting access to the emerging plasma membrane; this was successfully done in *Aspergillus* (Roberts et al., 1997) and *N. crassa* (Very & Davis, 1998). In both methods, the cells must be plasmolyzed and are thus far removed from their normal physiological state.

The *slime* mutant of *Neurospora crassa* is a cell wall-less strain (*fz*; *sg*; *os-1*) (Emerson, 1963), in which the plasma membrane is directly accessible to the patch-clamp pipette. The mutant exhibits spheroplast cells, which have an amoeboid motility (Trevithick & Galsworthy, 1977; Heath & Steinberg, 1999). The cells lack the major components of cell wall, but still show the presence of poly- and monosaccharides on the plasma membrane surface (Trevithick & Galsworthy, 1977; Scarborough, 1988; Heath & Steinberg, 1999). In spite of the absence of light-regulated developmental stages in the *slime* mutant, the strict blue light regulation of the biosynthesis of carotenoids (except for ß-carotene) and the characteristics of photoinduced carotenogenesis in the mutant are identical to wild type (Mitzka & Rau, 1977). Therefore, the *slime* mutant offers unique advantages for application of the patch-clamp technique to study membrane-associated processes evoked by BL.

To identify the specific ion fluxes, we used the ion-selective vibrating probe technique (Lucas & Kochian, 1986; Newman et al., 1987; Kuhtreiber & Jaffe, 1990), which has been successfully used to identify ion fluxes in growing hyphae (Lew, 1999) and light-induced ion flux changes in higher plants (Shabala & Newman, 1999). In this study we demonstrate that BL causes changes in the ionic conductance of the plasma membrane of the *slime* mutant of *Neurospora crassa*.

Materials and Methods

Cells

The cell wall-less *Neurospora crassa* mutant strain (*fz*; *sg*; *os-1*), *slime* (FGSC # 1118) was obtained from G. Scarborough (University of North Carolina, USA). Stock cultures were stored on agar slants (Bowman & Slayman, 1977) in the dark at room temperature. To maintain the cultures, every 7–10 days a liquid culture, Vogel's N medium (Vogel, 1956), supplemented with 2% mannitol (w/v), 0.75% yeast extract (w/v), and 0.75% nutrient broth (w/v), was inoculated from a slant culture, incubated for 24 hours at 30°C to OD_{600} 0.6–0.8, and a 75-µl aliquot was used to inoculate a new slant. For experiments, cells from slant cultures were inoculated in 30 ml of the same liquid medium and grown overnight (approximately 20 hrs) in the shaker (50 rpm) at 30°C. In the morning, 100 µl of the culture was transferred into 30 ml of medium of identical

composition, grown as before and after 3–5 hours of growth, cells were used for experiments. For patch-clamp experiments, 1 ml of the culture was centrifuged at 5,600 × g for 5 sec, washed twice with bath solution (BS) (in mM: 50 KCl, 50 $MgCl_2$, 1 $CaCl_2$, 10 MES/BTP, pH 5.8, adjusted with sorbitol to total osmolality 390 mosmol/kg), and resuspended in 1 ml of BS. Cells (20 μl) were transferred into the experimental chamber containing 2 ml of BS. Cells used for patching were of variable size, with diameter between 8 and 25 μm. We chose non-vacuolated, initially spherical cells, which became amoeba-like after they attached to the bottom, but did not form pseudopodia. Seals were usually achieved within 5–10 min after the patch pipette was pressed against the cell surface and the initially applied positive pressure was released. Due to cell motility, seals spontaneously disrupted within 5–10 min.

Growth and all manipulations with cells were performed under a red safe light of low intensity (2×10^3 μW/cm^2).

Cells were viewed with Nomarski differential contrast optics (60 × water immersion objective, Zeiss Axioscope2 microscope, Jena, Germany). Cells were patched under red light (interference filter 610 nm, 10-nm bandpass, Optometrics, USA) at an intensity of 2.6×10^3 μW/cm^2. The red filter was manually replaced with a blue filter (interference filter 467 nm, 10-nm bandpass) and intensity adjusted to 2×10^3 μW/cm^2. In experiments with the vibrating ion-selective probe, a blue filter C-99 (470 nm, 130-nm bandpass, AGFA-Gavaert, Belgium) was used together with an underlying container filled with 2% $CuSO_4$. The light intensity was measured with a radiometer (268R detector attached to a 350 radiometer; United Detector Technology, USA).

Electrophysiology

Membrane currents were measured using the whole-cell configuration of the patch-clamp technique (Hamill et al., 1981). We employed the nystatin-perforated whole-cell patch-clamp method (Horn & Marty, 1988; Strauss et al., 2001). Nystatin (400 μg/ml from a DMSO stock, final DMSO concentration 0.2%) was present in the pipette solution (PS) (in mM: 50 KCl, 1 $MgCl_2$, 1 $CaCl_2$, 5.5 EGTA, 10 HEPES/BTP pH 7.2, no sorbitol, free [Ca^{2+}] 10^{-8} M). The patch-pipette resistance in 50 mM KCl BS was 20 MΩ. Pipettes were pulled from borosilicate capillary tubes (standard wall with filament) (Warner Instrument, USA) on a vertical puller (P-30, Sutter Instruments, USA). After the seal resistance reached approximately 500 MΩ, a negative voltage of −40 mV was applied to the pipette to facilitate the formation of the gigaOhm (GΩ) seal. Typically, seal resistances ranged between 2–5 GΩ. We did not perform the leak subtraction procedure, so as not to discard linear components of ion-selective conductance. The capacitance of the cell was usually apparent within 3–5 minutes after seal formation, as nystatin diffused to the pipette tip and perforated the patch (Marty and Neher, 1995).

Membrane currents and potential were recorded with a Dagan patch-clamp amplifier (Model 8900, Dagan, USA). We used an agar salt bridge with [KCl] matching pipette [Cl^-] to minimize junction potentials. We recorded the total voltage, which includes the holding potential and the voltage required to compensate for the liquid junction potential (if any), so we knew the actual voltage in the pipette. The voltages shown in the *I-V* plots are the pipette voltages corrected for the junction potential. Currents were filtered at 200 Hz or 2 kHz, depending on the protocol, with a low-pass Bessel Filter (model LPF-100B, Warner Instruments, USA), and digitized with a Digidata 200 (Axon Instruments, USA) at a sample frequency of 1 or 5 kHz. Data acquisition and analysis were performed using pClamp 6.0 software (Axon Instruments) and Sigma Plot and SYSTAT statistical software (SPSS Science, USA). Data were directly stored on a computer hard disk. Data are shown as mean ± SE, n = sample size.

In our whole-cell experiments the sign convention was that negative membrane voltages mean cytoplasmic electric potential negative to the apoplastic electrical potential, and negative shift in the command voltage causes a negative shift in membrane voltage and is hyperpolarizing. Whole-cell negative currents mean inward flow of positive charges into the cell (and pipette) from external solution. We present currents at positive, near zero, and negative voltages, since blue light effects could be more prominent at certain voltages depending upon which ion transporters are affected.

To measure membrane potential, we used standard glass micropipettes (tip diameter 0.05 μm) filled with 1 M KCl; the amplifier and software were then used in current-clamp mode. Cells were impaled in 50 mM KCl BS.

Ion Flux Measurements

Net fluxes of H^+, K^+, Ca^{2+} and Cl^- were measured non-invasively using ion-selective vibrating microelectrodes (the MIFE™ technique; University of Tasmania, Hobart, Australia). Specific details on microelectrode fabrication and calibration are available from previous publications (Shabala, Newman & Morris, 1997; Shabala & Newman, 1999; Shabala, Babourina & Newman, 2000). A modified version of the MIFE setup, using an upright microscope and providing for the cell to be immobilized on a cover slip or bottom of a Petri dish, was employed (*see* Shabala et al., 2001a for details). Commercially available ionophore cocktails (Fluka catalog numbers 95297 for H^+, 60031 for K^+, 24902 for Cl^- and 21048 for Ca^{2+}) were used. The electrodes were calibrated in sets of standards before and after use. Electrodes with a response of less than 25 mV per tenfold concentration difference for Ca^{2+}, and 50 mV for H^+, K^+, and Cl^-, were discarded. Ion fluxes were measured from cells bathed in the external solutions with low concentrations of each ion under study (in order to increase the signal to noise ratio); the composition of external solutions was as follows: for H^+—10 mM KCl, 1 mM $CaCl_2$, 1 mM $MgCl_2$, pH 5.5 (unbuffered); for K^+—50 μM KCl, 1 mM $CaCl_2$, 1 mM $MgCl_2$; [K^+] = 50 μM, [Cl^-] = 4.05 mM; for Cl^-—50 μM $CaCl_2$, 50 μM $MgCl_2$, 100 μM KCl; [Cl^-] = 300 μM; [K^+] = 100 μM; for Ca^{2+}—50 μM $CaCl_2$, 180 mM KCl, 50 μM $MgCl_2$; [Ca^{2+}] = 50 μM. Solutions for K^+, Cl^-, and Ca^{2+} were buffered to pH 5.8 with 5 mM HEPES, and all solutions contained appropriate volumes of 1 M sucrose to adjust osmolality.

Ion fluxes were measured in the steady state for 5 to 10 min and then the blue light treatment was given. The sampling rate was 15 Hz, and the frequency of the electrode movement was 0.1 Hz. As most cells exhibited a high degree of motility, special attention was paid to maintain a constant distance between the ion-selective probe and the *slime* cell. The distance was periodically (every 1 min) checked and adjusted, using a 3D-hydraulically driven micromanipulator. Spherical geometry diffusion was used to calculate net fluxes of the measured ions essentially as reviewed by Newman (2001).

Spectral analysis of ion flux oscillations was performed as described in Shabala & Newman (1999) by applying the Discrete Fourier Transform (DFT) using EXCEL 4.0 package. Using the IMABS tool in EXCEL 4.0, the moduli of the complex amplitudes were returned from the DFT spectra. These moduli were later plotted against the period (T) of the harmonic components for the discrete frequencies $v = 0, 1/T, 2/T, \ldots, (n-1)/T$.

Drugs

In some experiments, $BaCl_2$ or tetraethylammonium (TEA) was added to the BS to block K^+ channels, and 4,4′-diisothiocyanostilbene-2, 2′-disulfonic acid (DIDS), to block anion channels.

Nystatin, TEA and other chemicals were purchased from Sigma-Aldrich. Inhibitors were added from stocks directly to the experimental chamber with a micropipette. Inhibitors were washed out by perfusion of the chamber using a peristaltic pump (flow rate 1 ml/min).

Measurement of Intracellular Potassium Concentration

Intracellular concentration of potassium ions in *slime* cells was determined by atomic absorption spectrophotometry (Perkin-Elmer Atomic Absorption Spectrometer 3110, USA). Cells were grown as described for patch-clamp experiments, collected by centrifugation, washed twice with ice-cold dH_2O adjusted to isotonic osmolality with sorbitol. Cells were lysed in distilled water and potassium concentration in the lysate was determined by absorption at 404.4 nm. Calculations of intracellular potassium concentration were made based on the mean single-cell volume of 0.83 pLiters (based on perimeter and height measurements using Openlab, Improvision, UK) and on the number of cells per μl. The experiment was repeated twice.

Results

Patching *slime*

The *Neurospora crassa slime* mutant was first isolated and described by Emerson (1963). It is a unique example among fungal cells since it grows as wall-less spheroplasts. Although some polysaccharides are present on the cell surface, the lack of rigid cell wall permits direct access in vivo to plasma membrane without preliminary digestion of the cell wall, a procedure that probably leads to damage of subcellular structures involved in the regulation of the membrane processes under study. This was the major reason we chose the *slime* mutant for patch-clamp experiments. The *slime* mutant exhibits early blue light effects; the characteristics of the photo-induction of carotenoid biosynthesis in the *slime* cells are similar to those in the wild type (Mitzka & Rau, 1977). It is an ideal model system for analysis of BL effects on ionic transport.

When the *slime* cells are placed in the experimental chamber, they settle to the glass bottom, become flattened and perform slow amoeboid movements extending large blunt pseudopodia at a rate of about 5 μm/min, comparable to the rate of tip growth in *N. crassa* hyphae (Heath & Steinberg, 1999). Based on our observations, this motility is the main obstacle for keeping tight seals for a long time in patch-clamp experiments. In preliminary experiments, we immobilized the cells by pretreatment with concanavalin A (ConA) (0.2 mg/ml). ConA is a lectin, which crosslinks membrane glycoproteins and strongly inhibits the propagated growth of slime cells (Trevithick & Galsworthy, 1977). Although ConA prevented cell movements, getting stable high-resistance contact (GΩ seal) between the patch pipette and the cell membrane remained a problem, possibly due to the deformation of the cell membrane caused by cross-linking of membrane-associated components.

Another factor that impeded formation of GΩ seal contacts between the *slime* membrane and patch pipette is related to the peculiar properties of *slime* cell plasma membrane. When the patch pipette was pressed against the cell surface and negative pressure was applied to establish a GΩ seal, the plasma membrane readily penetrated into the pipette and the pipette tip was filled with a series of vesicles resembling a row of necklace "beads" (Fig. 1 *A–D*). With consistent suction, the whole cell was able to squeeze inside of the pipette (Fig. 1*F*). If the negative pressure was released, the "beads" retracted back and incorporated into the cell membrane (Fig. 1*C*, *D*), indicating that the "beads" had been connected with each other and with the cell by cytoplasmic bridges. Such flexibility of the plasma membrane may be due to the unusual lipid composition of the *slime* plasma membrane (Lampen, 1966; Trevithick & Galsworthy, 1977; Grindle & Farrow, 1978; Lakin-Thomas, Brody & Cote, 1997).

To minimize pressure application, we used the perforated whole-cell patch clamp method (Horn & Marty, 1988). This method employs the ability of the polyene antibiotic nystatin to form nonselective pores in sterol-containing membranes, such as fungal plasma membranes. In our experiments, the very tip of the pipette was filled with the regular PS and backfilled with PS containing 400 μg/ml of nystatin. The cell was patched immediately, before nystatin diffused into the pipette tip. When a GΩ seal was achieved, the cell was left for 5–10 min until nystatin incorporated into the membrane and the whole-cell configuration formed, as determined by the appearance of whole-cell capacitance (Marty and Neher, 1993).

It should be noted that a high concentration of Mg^{2+} in the bath was important for obtaining GΩ seals. High $[Mg^{2+}]$ is also a prerequisite for patching bacterial cells (Martinac et al., 1987). With lower concentrations of $MgCl_2$ we never observed a GΩ seal formation. Although only a few percent of the initially formed GΩ seals resulted in stable and long-lasting recordings, we were able to characterize whole-cell currents in some detail.

Whole-Cell Currents in *slime* Cells

Under control conditions (red or white light, PS 50 mM KCl, BS 50 mM KCl), application of a ramp voltage to the whole-cell membrane evoked currents that were virtually proportional to the transmembrane voltage in the range from about −100 to +100 mV. Total conductance of the membrane in this voltage range was 1.2 ± 0.2 nS (n = 8) (red

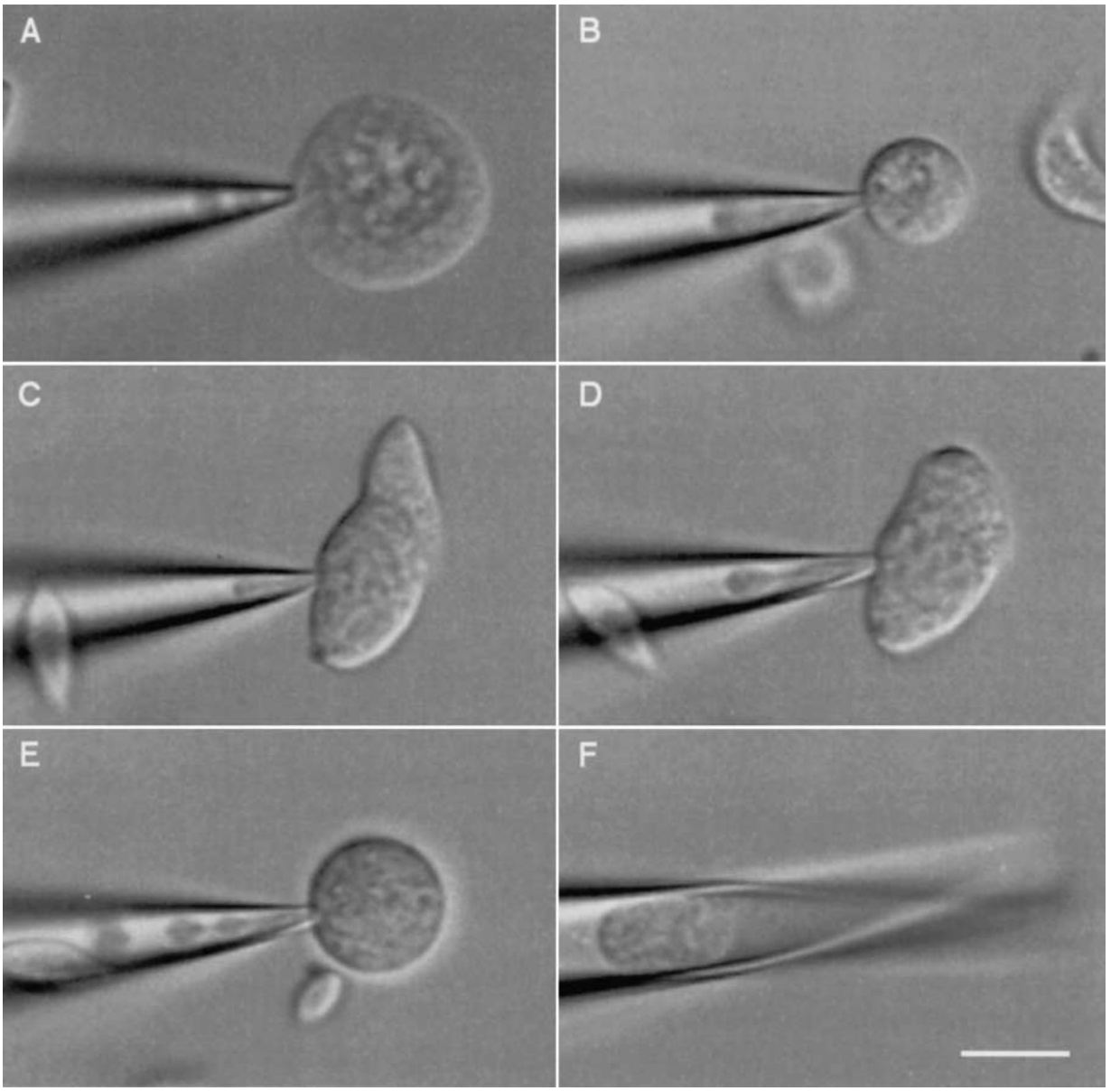

Fig. 1. Patch clamp procedure on *N. crassa slime* mutant cells. (*A*) Spontaneous flow of cell membrane vesicles (''beads'') into the patch pipette occurs when the pipette comes into contact with the cell surface and positive pressure is released. The ''beads'' are connected to each other by cytoplasmic bridges. (*B*) If suction is applied, more membrane vesicles enter the pipette. (*C*) When positive pressure is applied, the ''beads'' exit the pipette, and are reincorporated into the body of the cell. (*D*, *E*) Repeated application of suction causes the secondary formation of ''beads'' strings. (*F*) Occasionally, the whole cell was squeezed inside the pipette if the suction was maintained. Bar, 10 μm.

light experiments) (0.8 GΩ; the whole-cell conductance will dominate conductance measurements, since the whole-cell resistance is much less than the in-parallel seal resistance). At voltages more negative than −100 mV and more positive than 100 mV, the slope conductance was slightly higher than in the linear area. (This rectification of inward and outward currents was observed beyond biologically relevant voltages and may be due to instability of the seal.) Figure 2*A* shows current-voltage (I/V) relationships obtained upon application of a voltage ramp pulse (from −150 to +150 mV; 100 msec duration, holding potential −10 mV, 10 episodes) recorded under red light. Voltage ramps with increased duration (500 msec) gave the same I/V plots as the 100-msec voltage ramps. Similar I/V relations were obtained in experiments employing a voltage-step stimulation protocol. Figure 2*B* illustrates an I/V relationship for steady-state currents evoked by voltage steps applied from −150 to +130 mV (20-mV increments, duration of the step 250 msec, total duration 500 msec, holding potential −10 mV). To assess the effects of the blue

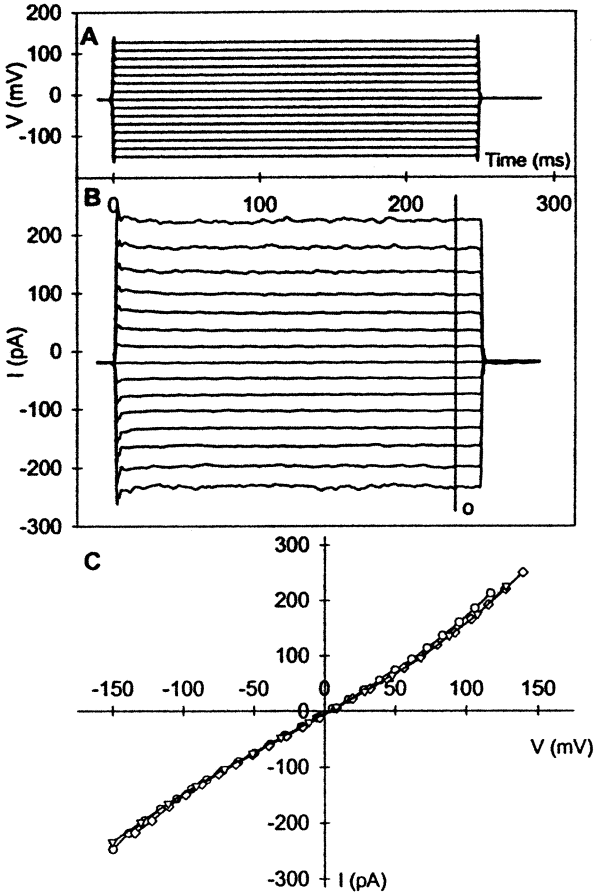

Fig. 2. Whole-cell currents measured with a voltage step-pulse protocol. Whole-cell membrane currents were recorded in standard extracellular solution with symmetrical KCl; BS (mM): 50 KCl, 1 $CaCl_2$, 50 $MgCl_2$, 10 MES/BTP, pH 5.8; PS (mM): 50 KCl, 1 $CaCl_2$, 5.5 EGTA, (free $[Ca^{2+}]$, 10^{-8} M), 1 $MgCl_2$, 10 HEPES/BTP, pH 7.2. The membrane potential was held at −10 mV, currents were measured at 240 msec in response to 250-msec pulses from −150 to +130 mV in 20-mV increments. (*A*) Voltage pulse-step protocol. (*B*) Currents evoked by step-voltage pulses. (*C*) I/V relationships obtained from different voltage pulse protocols. ○: from the step voltage pulse, current was measured at 240 msec, marked by straight line in *B*); ◊: from fast-ramp voltage-pulse (100 msec long, from −150 to +150 mV, 10 episodes in 400-msec intervals); ∇: from slow-ramp voltage-pulses (1 sec long, from −150 to +130 mV, 60 episodes in 2-sec intervals).

light and ion channel blockers we used voltage ramps mainly, as this experimental protocol allows monitoring of the changes of the whole-cell membrane currents at different voltages in a more compact time scale and is therefore more informative than the voltage-step protocol.

Effect of Blue Light on Whole-Cell Current

After the stable GΩ seal was established under red light, a number of fast-ramp voltage-pulse protocols were applied to the cell, and then, during a slow-ramp voltage-pulse protocol with 60 episodes, the light was switched from red to blue on episodes 10–20. We recorded data for the 3.5-min time interval before the application of BL and for up to 5 min after the onset of BL when the current came to a new steady state. Figure 3*A* shows the representative I/V relationships under red light and after application of blue light.

Table 1. Blue light-induced V_{rev} and current changes

Light	n	V_{rev} (mV)	ΔI ($\lvert I_t\rvert - \lvert I_0\rvert$) (pA) at V_m		
			+75 mV	−10 mV	−100 mV
Red	8	−10 ± 7	−11 ± 4[a]	4 ± 2	0 ± 7[b]
Blue	6	−24 ± 13	−31 ± 5[a]	−2 ± 2	−44 ± 6[b]

n, number of experiments
[a] significantly different; t-test, $P = 0.025$
[b] significantly different; t-test, $P = 0.003$

Most cells (6 cells out of 8) showed a decrease in inward and outward currents under blue light illumination (2 out of 8 cells showed only decreased outward current, but increased inward current). Two cells (out of 6) showed slight changes in conductance within 40 sec of blue light, but the most pronounced effects were detectable after 2–4 min for all cells. We plotted the time course of the currents at −100 and +75 mV, i.e., at voltages where the changes of current were most pronounced, and at −10 mV, near the reversal potential, V_{rev} (Fig. 3). To evaluate the change in current we calculated the difference between the current recorded at time 0 (I_0) and the current recorded 2–3 min after the onset of the BL illumination (I_t); the delta I was calculated as $\Delta I = |I_t| - |I_0|$, where a negative sign of ΔI reflects the decrease of outward and inward currents. Under red light the spontaneous change of clamping currents was very small over the 3–4-min period. Blue light caused significant decline in both the inward and outward currents over the 3–4-min period (Table 1). The total conductance (slope of I/V curve) decreased from 1.5 ± 0.3 nS to 1.2 ± 0.4 nS, $n = 6$ ($P = 0.01$, paired t-test).

Figure 3*A* shows the representative I/V relationships before (open circles) and after (closed circles) application of BL. A decrease in the amplitude of both inward and outward current could be detected immediately after application of BL (Fig. 3*D*). The change reached its steady state after 3–4 min. Figure 3*C* shows the time course of BL effect of currents at −100, −10 and +75 mV.

To identify the ion fluxes required for the conductance changes, we examined BL effects on the reversal potential. The value of V_{rev} under red light, as well as the magnitude of membrane potential shift induced by blue light, varied, but the direction of the change was consistent: V_{rev} shifted towards negative values (Fig. 3*B*). Under red light, at symmetrical

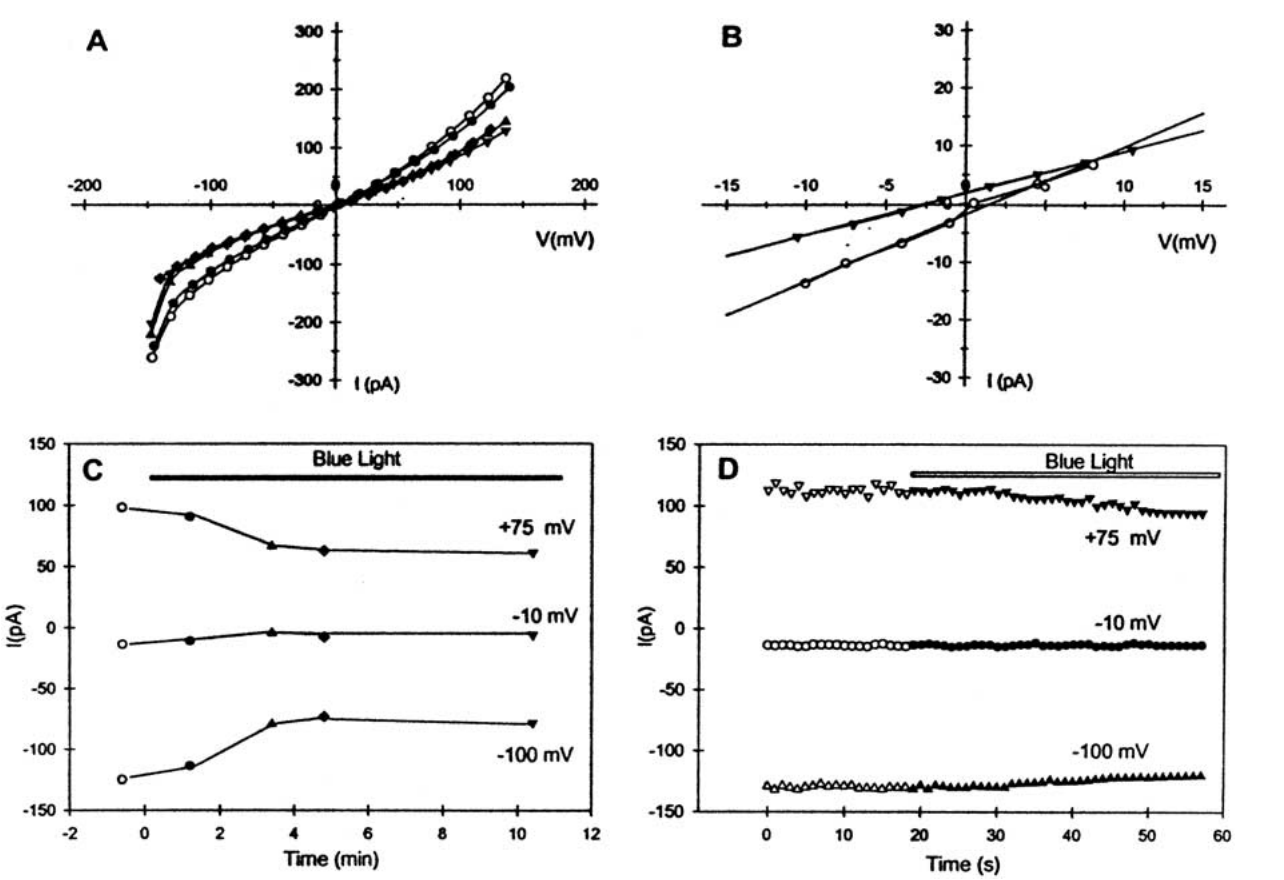

Fig. 3. BL-induced changes in whole-cell currents. (*A*) *I*/*V* relationships obtained from fast-ramp-voltage pulse before (open symbols) and after (closed symbols) application of BL. (○) Under red light, (●) 1.2 min after BL application, (▲) 3.4 min BL, (♦) 4.8 min BL, (▼) 10.4 min. (*B*) BL-induced shift of V_{rev} (enlarged from *A*), linear regression approximation for V_{rev} RL = 2 mV, V_{rev} BL = −3 mV. G_{RL} = 1.2 nS, G_{BL} = 0.7 nS. (*C*) Time course of BL effect on whole-cell currents, the current amplitude of the inward current at membrane potential of −100 mV and −10 mV, and the current amplitude of the outward current at membrane potential of +75 mV are plotted. Symbols correspond to *I*/*V* curves on panel *A*. (*D*) Time course of whole-cell currents, induced by slow-ramp voltage pulse, and recorded immediately before and after BL application. The measurements were made in a standard extracellular solution with symmetrical KCl; BS (mM) 50 KCl, 1 $CaCl_2$, 50 $MgCl_2$, 10 MES/BTP, pH 5.8; PS (mM): 50 KCl, 1 $CaCl_2$, 5.5 EGTA, (free $[Ca^{2+}]$ 10^{-8} M), 1 $MgCl_2$, 10 HEPES/BTP, pH 7.2, 400 μg/ml nystatin.

50-mM KCl concentrations in BS and PS, V_{rev} was −10 ± 7 mV (n = 8), (range: −43 mV to +6 mV). Under blue light, V_{rev} was −24 ± 13 mV (n = 6), (range: −61 to 0 mV). The spontaneous change of V_{rev} under RL was +6.6 ± 4 mV (n = 6) for a period of up to 4 min. Blue light caused V_{rev} to shift in the negative direction (hyperpolarization). In 4 out of the 6 cells that demonstrated the decrease in total conductance in response to BL, the change in V_{rev} was −9 ± 4 mV over the same period. There was no change in V_{rev} for one cell (V_{rev}(RL)−V_{rev}(BL)∼ −2 mV). There was a positive shift from −11 mV to −7 mV in one cell, for which the bath solution contained 50 mM KCl and the pipette 150 mM KCl. The positive shift of V_{rev} in asymmetric KCl is consistent with the data for the other 4 cells if the decrease in conductance is due to a decrease in K^+ conductance, so that the V_{rev} shifts to the E_{Cl^-}, which for BS/PS = 50/150 mM KCl is 0 mV, while E_{K^+} is −28 mV.

Reversal Potential and Intracellular Membrane Potential Measurements

To identify the components contributing to the observed whole-cell conductance, we determined reversal potentials at different concentrations of K^+ and Cl^- in the bath (the KCl concentration in the pipette solution was always 50 mM). In BS containing 50 mM KCl and 50 mM $MgCl_2$, current reversed at approximately −10 ± 2 mV (n = 4). When KCl concentrations in the bath were 5 and 100 mM (there was 50 mM $MgCl_2$ in BS), reversal potentials were, respectively, −39 ± 16 mV (n = 4) and −11 ± 1 (n = 5). For each solution, we compared V_{rev} to the Nernst potentials for K^+ and Cl^-, calculated based on ion activities for the given ion gradients. The data are summarized in Table 2.

At $[K^+]$ in the bath below 50 mM, V_{rev} correlated linearly with log $[K^+]_{out}$, so that a tenfold decrease in

Table 2. Experimental V_{rev} and estimated Nernst potentials E for *slime* cells

$[K^+]_{in}$ mM	$[K^+]_{out}$ mM	E_{K^+} mV	$[Cl^-]_{in}$ mM	$[Cl^-]_{out}$ mM	E_{Cl^-} mV	V_{rev} mV	n
50	100	+15	54	202	−30	−11 ± 1	5
50	50	0	54	152	−23	−10 ± 2	4
50	5	−52	54	107	−17	−42 ± 16	4

$[K^+]_{out}$ shifted V_{rev} towards more negative voltages by 32 mV. If the membrane were permeable only to K^+, the shift would have been −52 mV. This discrepancy indicates that the potassium conductance is not the only component determining V_{rev}. The data suggest that the membrane is also Cl^- permeable. Indeed, under symmetrical $[K^+]$ conditions, $V_{rev} = \sim -10$ mV, not zero as predicted by the Nernst equation for K^+. Under the same conditions, the Nernst potential for Cl^- was −23 mV, which may well account for the observed value of V_{rev} of −10 mV.

The membrane potential recorded in intact *slime* cells with an intracellular microelectrode was −14 ± 2 mV (n = 5) with 50 mM KCl in the bath; potentials of a similar magnitude have been reported in other amoeboid cells (Bingley, 1966; Braatz-Schade, Haberey, Stockem, 1973). Based on experiments in which the micropipette tip contained a fluorescent tracer dye (lucifer yellow), the tip was located in the cytoplasm (Fig. 4). The potential was stable for about a second and then gradually depolarized. To estimate the contribution of different ions to generation of the membrane potential, we determined the intracellular $[K^+]$ by absorption spectroscopy. $[K^+]_{in}$ was about 20 mM. Similar values (35 mM) have been reported for *Dictyostelium discoideum* (Schlatterer et al., 1994). Intracellular $[Cl^-]$ was reported to be 10 mM in *N. crassa* spheroplasts (Blatt & Slayman, 1983), and 0.2 mM for hyphal cells (Slayman, 1965). We can assume that the intracellular $[Cl^-]$ in *slime* cells is around 20 mM or higher, since $[Cl^-]$ in the bath is 152 mM. Providing that membrane potential (E_m) is determined by K^+ and Cl^- conductance only, we can make approximate estimates of the $g = G_{K^+}/G_{Cl^-}$ ratio. Since

$$E_m = (E_{K^+}g + E_{Cl^-})/(1+g), \text{ then}$$

$$g = (E_m - E_{Cl^-})/(E_{K^+} - E_m)$$

For $[K^+]_{out} = 50$ mM and $[K^+]_{in} = 20$ mM, $E_{K^+} = +22$ mV.

For the BS containing 50 mM KCl and 50 mM $MgCl_2$, $[Cl^-]_{out} = 152$ mM. If $[Cl^-]_{in}$ is 20 mM, then E_{Cl^-} would be −48 mV, so $g = (-14+48)/(22+14) = 34/36 \approx 1$, i.e., $G_{K^+} \approx G_{Cl^-}$. The presence of K^+ and Cl^- conductances was confirmed with channel inhibitors.

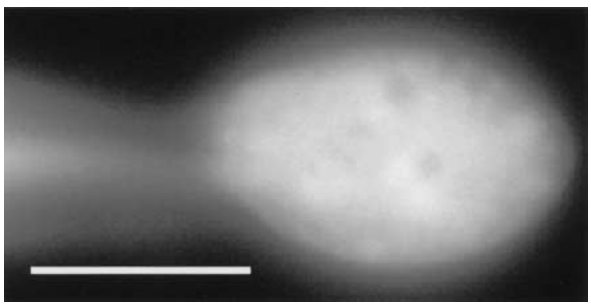

Fig. 4. Micropipette tip location during impalements under current clamp conditions. The micropipette tip was loaded with a fluorescent tracer, lucifer yellow. Upon impalement, the dye entered the cytoplasm of the cell (non-impaled surrounding cells, not visible in this fluorescence image, did not contain the tracer dye). Tip location in the cytoplasm has also been reported for other amoeboid cells, notably *Dictyostelium* (Van Duijn et al., 1988). An underestimate of the 'true' membrane potential may occur because of a shunt resistance at the impalement site. Bar = 10 μm.

Effects of Ion Channel Blockers On Whole-Cell Current

Whole-cell currents in *slime* were sensitive to common ion channel blockers. TEA (10 mM), a blocker of both inwardly and outwardly rectifying potassium channels (Khodakhah, Melishchuk & Armstrong, 1997), markedly suppressed the whole-cell currents in the voltage range between −100 and +100 mV within 15 sec. The total conductance (slope of the I/V curve) typically decreased about twofold; inhibition was reversible and the conductance was restored after the blocker was washed out (Fig. 5*A*). In addition to decreasing conductance, TEA shifted the reversal potential towards E_{Cl^-} (Fig. 5*C*). Thus, under the symmetrical conditions for $[K^+]$ (50 mM KCl in bath and pipette solutions), TEA produced a negative shift of the reversal potential by 6 to 14 mV. When TEA was applied to the cell bathed in 5 mM KCl, V_{rev} shifted to more positive voltages from −54 to −20 mV—again, closer to E_{Cl^-} (*see* Table 2). The difference I/V relationships for the TEA-sensitive current are shown in Fig. 5*B*, *D*. The TEA-sensitive current exhibited a V_{rev} of +2 mV; this value is close to the predicted equilibrium potential for K^+ ($E_{K^+} = 0$ mV).

Application of $BaCl_2$ (1 mM), a blocker of the inwardly rectifying potassium channel (Standen &

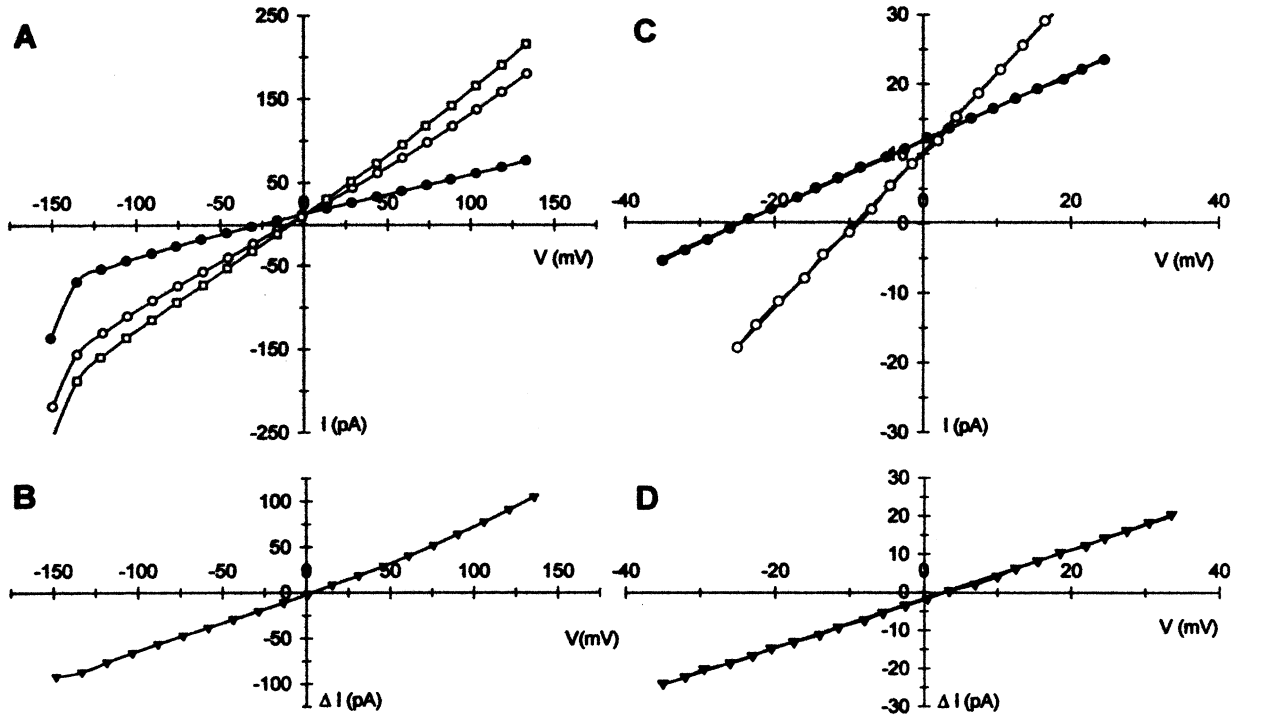

Fig. 5. Effect of 10 mM TEA on whole-cell currents. (*A*) *I*/*V* relationships obtained from fast-ramp voltage-pulse protocol. (○) Before addition of TEA, $t = -45$ sec (●) In the presence of TEA, $t = +45$ sec. (◊) After wash-out of TEA, $t = 2.5$ min. (*B*) (▼) The *I*/*V* relationship of the TEA-sensitive current. (*C*) The *I*/*V* relationship, enlarged from *A*, and showing the TEA effect on V_{rev}: (○) before the addition of TEA, $V_{rev} = -9$ mV; (●) in the presence of TEA, $V_{rev} = -25$ mV. (*D*) The *I*/*V* relationship, enlarged from *B*, and showing the $V_{rev} = 2$ mV for TEA-sensitive current. The measurements were made in a standard extracellular solution with symmetrical KCl; BS (mM): 50 KCl, 1 $CaCl_2$, 50 $MgCl_2$, 10 MES/BTP, pH 5.8; PS (mM): 50 KCl, 1 $CaCl_2$, 5.5 EGTA, (free $[Ca^{2+}]$ 10^{-8} M), 1 $MgCl_2$, 10 HEPES/BTP, pH 7.2.

Stanfield, 1978), decreased the slope conductance within 30 seconds. The effect was more pronounced for the inward current. V_{rev} shifted towards negative values, indicating that the Cl^- conductance dominates after the K^+ conductance is inhibited.

Application of the Cl^- channel blocker DIDS (200 μM) (Lin, 1981) inhibited outward and inward currents within 1 min. V_{rev} shifted only slightly to the negative voltages from −7 to −10 mV (in symmetrical conditions for $[K^+] = 50$ mM KCl in bath and pipette solutions.

Effect of Blue Light on Net Ion Fluxes from *slime* Cells

In separate experiments, kinetics of net ion fluxes from the *slime* cells was measured in response to blue light illumination. For optimal measurements, the concentration of the ion being measured was kept lower in the flux experiments than in patch-clamp measurements. Blue light caused significant changes in net H^+, K^+ and Cl^- fluxes across the plasma membrane of the *slime* cells, but had no impact on net Ca^{2+} flux (Fig. 6). The significant decrease in net H^+ influx and increase in net Cl^- influx and K^+ efflux were detectable a few minutes after the BL treatment (Fig. 6*A*, *B*, *C*). The time course of response was similar for all ions. An important feature of these responses was their reversibility. When the BL was changed back to red, the fluxes reversed (Fig. 6, upper panels), with variable time courses, from immediate to 10 to 15 min, and approached their initial values. Under constant red light illumination, ion fluxes from *slime* cells oscillated slightly around a base line, but remained steady for at least 30–40 min of experiment (illustrated for H^+; open circles in Fig. 6*A*).

Fast oscillations in all net ion fluxes were observed in *slime* under RL and BL (Fig. 6, period is about 1 min), but not in measurements distant from the cell (*data not shown*). Oscillations in net ion fluxes are common in plants (Messerli, Danuser & Robinson, 1999; Shabala et al., 2001b) and membrane potential oscillations were reported in the *N. crassa poky* mutant (induced by cyanide; Gradmann & Slayman, 1975). Because they are independent of BL effects, we did not examine them in detail.

Discussion

In this study we demonstrated that blue light illumination of *N. crassa slime* mutant cells causes changes

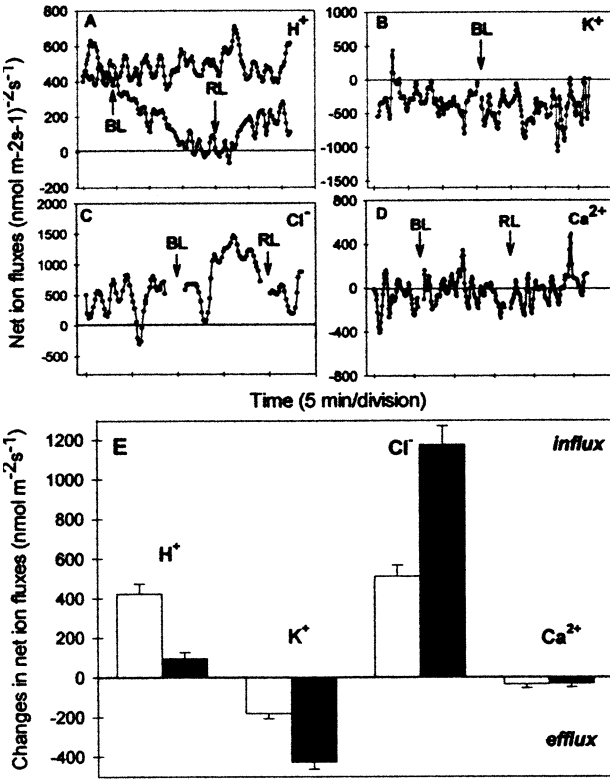

Fig. 6. BL-induced ion flux kinetics recorded in MIFE experiments. Light-induced changes in net H^+ (*A*), K^+ (*B*), Cl^- (*C*), and Ca^{2+} (*D*) fluxes (inward positive) measured in response to blue (BL) and red (RL) light treatments (as marked). (*E*) Average values of net H^+, K^+, Cl^- and Ca^{2+} fluxes before (white bars) and 5 min after (black bars) blue light treatment. Error bars are SE ($n = 4$). Composition of external solutions was as follows: for H^+—10 mM KCl, 1 mM $CaCl_2$, 1 mM $MgCl_2$, pH 5.5 (unbuffered); for K^+—50 μM KCl, 1 mM $CaCl_2$, 1 mM $MgCl_2$; for Cl^-—50 μM $CaCl_2$, 50 μM $MgCl_2$, 100 μM KCl; for Ca^{2+}—50 μM $CaCl_2$, 180 mM KCl, 50 μM $MgCl_2$. Solutions for K^+, Cl^-, and Ca^{2+} were buffered to pH 5.8 with 5 mM HEPES, and all solutions contained appropriate volumes of 1 M sucrose to adjust osmolality.

in the electrical properties of the plasma membrane within 2–4 min. In the majority of patch-clamp experiments, a decline in conductance is accompanied by a negative shift of the reversal potential reflecting the hyperpolarization of the plasma membrane. Both observations are in agreement with previously reported BL-induced changes in the membrane resistance and membrane potential of *N. crassa* hyphae (Potapova et al., 1984). Furthermore, our data showed that the change in the total conductance begins within a few seconds after the onset of blue light. The rapidity of the electrical changes caused by BL illumination suggests that these changes may be part of initial signal transduction.

In addition to conductance and reversal potential measurements, we used the ion-selective probe to identify changes in net ion fluxes after BL illumination. Within about 2–4 min of BL treatment, K^+ efflux increased, Cl^- influx increased, H^+ influx decreased, while Ca^{2+} flux remained unchanged.

To discuss the data obtained by two methods, we need to emphasize that these methods measure the ion transport across the membrane differently. In the case of whole-cell conductance measurements, the internal and external K^+ and Cl^- concentrations are defined. In the case of external net ion flux measurements, low external [K^+] and [Cl^-] are required to maximize the signal to noise ratio. Whole-cell ion conductance was measured over a wide range of voltages, while the ion-selective probe measures net ion fluxes at the resting potential of the cell. The total net charge movement, calculated from data on ion fluxes for H^+, K^+, Ca^{2+} and Cl^-, was about 13.9 pA during red light, and 15.6 pA after BL illumination, assuming a cell of 8 micron diameter. The change in current is similar to the one observed in whole-cell measurements at resting potential (Fig. 3*B*) and would be sufficient to explain the hyperpolarization of the membrane.

In the whole-cell measurements, BL-induced decline in conductance is attributed to the decrease in K^+ conductance. Under these circumstances, Cl^- conductance becomes dominant, resulting in a shift in the reversal potential towards E_{Cl^-} (under symmetrical [K^+], Table 2). Plasma membrane hyperpolarization may develop as a result of the decrease in K^+ inward current; activation of the H^+ pump could also account for part of the effect. This is consistent with the decline in net H^+ influx observed in ion-selective probe measurements, where net H^+ influx is defined as the sum of two components: the influx due to H^+/substrate symport activity (I_{o-i}) and efflux due to H^+ pump activity (I_{i-o}), described by the equation $I_{net} = I_{i-o} - I_{o-i}$. Therefore, increased extrusion of H^+ by the pump would result in decreased net H^+ influx. BL-induced hyperpolarization of plasma membrane was also observed in *Vicia faba* guard cells and *Phycomyces* hyphae, where it was demonstrated that proton pump activation is responsible for the hyperpolarization (Assmann et al., 1985; Weiss & Weisenseel, 1990; Kinoshita & Shimazaki, 1999).

The BL-induced increases in net K^+ efflux and Cl^- influx were observed under conditions of low external [K^+] and [Cl^-] (50 μM and 200 μM, respectively). For the increased Cl^- influx, there is no doubt that transporters separate and distinct from a Cl^- channel must be operating, since the driving forces will not allow electrophoretic uptake of Cl^- through a channel, because of the negative resting potential at low external [K^+] (estimated to be −127 mV at 100 μM, in the case of Cl^- flux measurements). To explain the increase in Cl^- influx we propose that a cation/chloride transporter exists in the plasma membrane of *slime* cells. This transporter may be activated under BL (directly or secondarily via plasma membrane hyperpolarization) so that, simultaneously

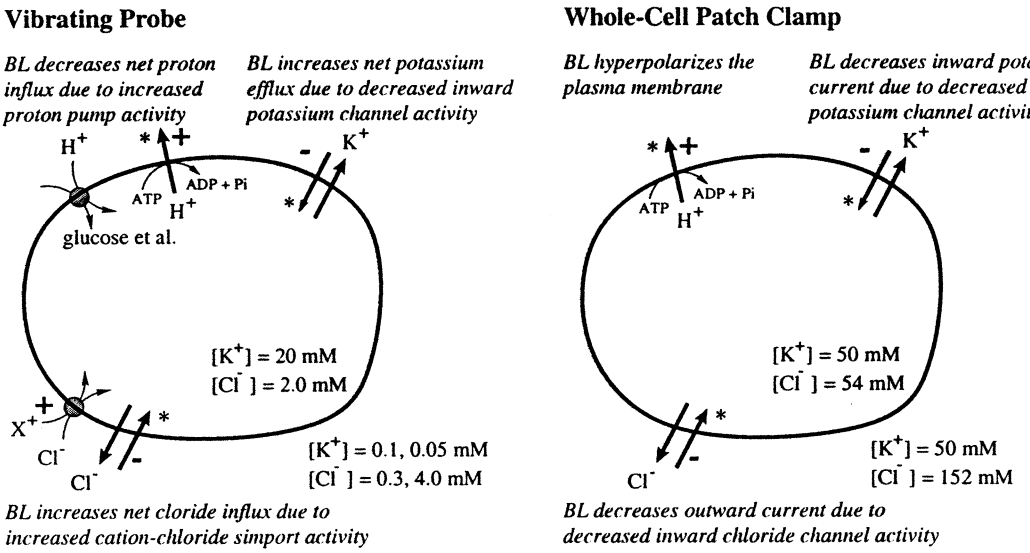

Fig. 7. BL effects on ion transport in *slime*. *indicates currents for which the changes coincide in both net ion flux and patch clamp experiments. "+" and "–" indicate activation and inhibition, respectively.

with decrease in outward current due to either a decrease in K^+ efflux or Cl^- influx, its activation will lead to the observed increase in net Cl^- influx. There is indirect evidence for the presence of a cation/chloride transporter in *N. crassa*. The genome contains a sequence (contig 2.203) with 30% identity and 49% similarity over 567 amino acids to a cation/chloride cotransporter from *Nicotiana tabacum* (accession # AAC49874) (BLAST search) (Neurospora Sequencing Project. Whitehead Institute/MIT Center for Genome Research [www-genome.wi.mit.edu]). Such a cotransporter could account for the increased Cl^- influx.

From our results we can conclude that BL regulation of electrogenic ion transport in *N. crassa* is complex; decreases in both K^+ and Cl^- channel activity are likely to occur and proton pump activity may be activated. A speculative summary of BL effects is shown in Fig. 7. Considerable research will be required to unravel each of the many putative regulatory effects blue light has on plasma membrane ion transport.

Our observations differ from those on higher plants, in which BL activates anion channels and depolarizes the plasma membrane. Electrophysiological studies on *Arabidopsis* and cucumber hypocotyls revealed that BL activates anion channels in plasma membrane (Spalding & Cosgrove, 1992; Cho & Spalding, 1996; Lewis et al., 1997); other evidence for anion channel activation by BL comes from inhibitor studies of BL-induced protoplast shrinking (Wang & Iino, 1997, 1998) and BL hypocotyl growth inhibition (Parks, Cho & Spalding, 1998).

Along with Cl^-, K^+, another major osmotically active ion in plants, is involved in a number of BL responses, such as *Vicia faba* stomatal guard cell swelling and *Arabidopsis* hypocotyl protoplast shrinkage (Satter & Galston, 1981; Assmann, 1993). Wang and Iino (1998) suggested that activation of outward-rectifying K^+ channels is involved in the BL-regulated mechanism of protoplast shrinkage, consistent with reports on BL-induced K^+ efflux in pulvinus flexor cells in *Samanea* (Suh et al., 2000) and *Phaseolus* (Okazaki, Azuma & Nishizaki, 2000). Suh et al. (2000) presented evidence that the BL activation of K^+ efflux channels occurs through both the E_m (depolarization) and an independent signaling pathway. The *slime* mutant, on the other hand, is not a cell specialized for turgor-active volume regulation, so it should not be surprising that channel regulation is different. What is surprising is the complexity of conductance and flux changes associated with BL illumination in this lower eucaryote, and the rapidity of the response.

The involvement of Ca^{2+} in blue-light signaling is well documented in both higher (Shinkle & Jones, 1988; Gehring et al., 1990; Baum et al., 1999; Guo et al., 2001; Long & Iino, 2001) and lower (Pu & Robinson, 1998) plants. However, we are not aware of direct evidence for a role of Ca^{2+} in BL responses in fungi, except for *Phycomyces*, in which it was shown that Ca^{2+} and calmodulin are involved in phototropism (Sineshchekov & Lipson, 1992; Valenzuela & Ruiz-Herrera, 1989). Since increased cytosolic Ca^{2+} is known to activate the H^+ pump in *N. crassa* (Lew, 1989), the observed hyperpolarization may result from the Ca^{2+} activation of the pump. However, we found no significant effect of BL on net Ca^{2+} flux across the plasma membrane of *slime* cell. Therefore, if Ca^{2+} is involved in the mediation of the

BL-induced signaling in *Neurospora*, it must be coming from internal stores, which would be similar to the internal supply of Ca^{2+} during apical growth (Silverman-Gavrila & Lew, 2001) and Ca^{2+} release from an intracellular store induced by blue light in *Arabidopsis* (Long & Jenkins, 1998).

This work was supported by NSERC and NATO Collaborative Linkage (#565370) grants to R.R. Lew and an NSERC grant to I.B. Heath. We thank Dr. I.B. Heath for stimulating discussions. We greatly appreciate the technical assistance of Karen Rethoret and John Currell.

References

Ahmad, M., Cashmore, A.R. 1993. HY4 gene of *A. thaliana* encodes a protein with characteristics of a blue-light photoreceptor. *Nature* **366:**162–166

Ahmad, M., Cashmore, A.R. 1996. Seeing blue: the discovery of cryptochrome. *Plant Mol. Biol.* **30:**851–861

Ahmad, M., Jarillo, J.A., Smirnova, O., Cashmore, A.R. 1998a. The CRY1 blue light photoreceptor of *Arabidopsis* interacts with phytochrome A in vitro. *Mol. Cell* **1:**939–948

Ahmad, M., Jarillo, J.A., Smirnova, O., Cashmore, A.R. 1998b. Cryptochrome blue-light photoreceptors of *Arabidopsis* implicated in phototropism. *Nature* **392:**720–723

Assmann, S. 1993. Signal transduction in guard cells. *Annu. Rev. Cell Biol.* **9:**345–375

Assmann, S.M., Simoncini, L., Schroeder, J.I. 1985. Blue light activates electrogenic ion pumping in guard cell protoplasts of *Vicia faba*. *Nature* **318:**285–287

Bagnall, D.J., King, R.W., Hangarter, R.P. 1996. Blue-light promotion of flowering is absent in hy4 mutants of *Arabidopsis*. *Planta* **200:**278–280

Ballario, P., Macino, G. 1997. White collar proteins: PASsing the light signal in *Neurospora crassa*. *Trends Microbiol.* **5:**458–462

Ballario, P., Vittorioso, P., Magrelli, A., Talora, C., Cabibbo, A., Macino, G. 1996. White collar-1, a central regulator of blue light responses in *Neurospora*, is a zinc finger protein. *EMBO J.* **15:**1650–1657

Baum, G., Long, J.C., Jenkins, G.I., Trewavas, A.J. 1999. Stimulation of the blue light phototropic receptor NPH1 causes a transient increase in cytosolic Ca^{2+}. *Proc. Natl. Acad. Sci. USA* **96:**13554–13559

Bertl, A., Slayman, C.L. 1992. Complex modulation of cation channels in the tonoplast and plasma membrane of *Saccharomyces cerevisiae*: single-channel studies. *J. Exp. Biol.* **172:**271–287

Bingley, M.S. 1966. Membrane potentials in *Amoeba proteus*. *J. Exp. Biol.* **45:**251–267

Blatt, M.R., Slayman, C.L. 1983. KCl leakage from microelectrodes and its impact on the membrane parameters of a non-excitable cell. *J. Membrane Biol.* **72:**223–234

Bowman, B.J., Slayman, C.W. 1977. Characterization of plasma membrane adenosine triphosphatase of *Neurospora crassa*. *J. Biol. Chem.* **252:**3357–3363

Braatz-Schade, K., Haberey, M., Stockem, W. 1973. Correlation between membrane potential, cell shape, and motile activity in *Amoeba proteus*. *Exptl. Cell Res.* **80:**456–458

Briggs, W.R., Beck, C.F., Cashmore, A.R., Christie, J.M., Hughes, J., Jarillo, J.A., Kagawa, T., Kanegae, H., Liscum, E., Nagatani, A., Okada, K., Salomon, M., Rudiger, W., Sakai, T., Takano, M., Wada, M., Watson, J.C. 2001. The phototropin family of photoreceptors. *Plant Cell* **13:**993–997

Cashmore, A.R., Jarillo, J.A., Wu, Y.J., Liu, D. 1999. Cryptochromes: blue light receptors for plants and animals. *Science* **284:**760–765

Cho, M.H., Spalding, E.P. 1996. An anion channel in *Arabidopsis* hypocotyls activated by blue light. *Proc. Natl. Acad. Sci. USA* **93:**8134–8138

Christie, J.M., Reymond, P., Powell, G.K., Bernasconi, P., Raibekas, A.A., Liscum, E., Briggs, W.R. 1998. *Arabidopsis* NPH1: a flavoprotein with the properties of a photoreceptor for phototropism. *Science* **282:**1698–1701

Degli-Innocenti, F., Russo, V.E. 1984. Isolation of new white collar mutants of *Neurospora crassa* and studies on their behavior in the blue light-induced formation of protoperithecia. *J. Bacteriol.* **159:**757–761

Emerson, S. 1963. Slime, a plasmodioid variant of *Neurospora crassa*. *Genetica* **34:**162–182

Frechilla, S., Zhu, J., Talbott, L.D., Zeiger, E. 1999. Stomata from npq1, a zeaxanthin-less *Arabidopsis* mutant, lack a specific response to blue light. *Plant Cell Physiol.* **40:**949–954

Garrill, A., Jackson, S.L., Lew, R.R., Heath, I.B. 1993. Ion channel activity and tip growth: tip-localized stretch-activated channels generate an essential Ca^{2+} gradient in the oomycete *Saprolegnia ferax*. *Eur. J. Cell Biol.* **60:**358–365

Gehring, C.A., Williams, D.A., Cody, S.H., Parish, R.W. 1990. Phototropism and geotropism in maize coleoptiles are spatially correlated with increases in cytosolic free calcium. *Nature* **345:**528–530

Gradmann, D., Slayman, C.L. 1975. Oscillations of an electrogenic pump in the plasma membrane of *Neurospora*. *J. Membrane Biol.* **23:**181–212

Grindle, M., Farrow, R. 1978. Sterol content and enzyme defects of nystatin-resistant mutants of *Neurospora crassa*. *Mol. Gen. Genet.* **165:**305–308

Guo, H., Mockler, T., Duong, H., Lin, C. 2001. SUB1, an *Arabidopsis* Ca^{2+}-binding protein involved in cryptochrome and phytochrome coaction. *Science* **291:**487–490

Gustin, M.C., Martinac, B., Saimi, Y., Culbertson, M.R., Kung, C. 1986. Ion channels in yeast. *Science* **233:**1195–1197

Hamill, O.P., Marty, A., Neher, E., Sakmann, B., Sigworth, F.J. 1981. Improved patch-clamp techniques for high-resolution current recording from cells and cell-free membrane patches. *Pfluegers Arch.* **391:**85–100

Harding, R.W., Turner, R.V. 1981. Photoregulation of the carotenoid biosynthetic pathway in albino and white collar mutants of *Neurospora crassa*. *Plant Physiol.* **68:**745–749

Heath, I.B., Steinberg, G. 1999. Mechanisms of hyphal tip growth: tube dwelling amoebae revisited. *Fungal Genet. Biol.* **28:**79–93

Horn, R., Marty, A. 1988. Muscarinic activation of ionic currents measured by a new whole-cell recording method. *J. Gen. Physiol.* **92:**145–149

Huala, E., Oeller, P.W., Liscum, E., Han, I.S., Larsen, E., Briggs, W.R. 1997. *Arabidopsis* NPH1: a protein kinase with a putative redox-sensing domain. *Science* **278:**2120–2123

Khodakhah, K., Melishchuk, A., Armstrong, C.M. 1997. Killing K channels with TEA^+. *Proc. Natl. Acad. Sci. USA* **94:**13335–13338

Kinoshita, T., Shimazaki, K. 1999. Blue light activates the plasma membrane H(+)-ATPase by phosphorylation of the C-terminus in stomatal guard cells. *EMBO J.* **18:**5548–5558

Kuhtreiber, W.M., Jaffe, L.F. 1990. Detection of extracellular calcium gradients with a calcium-specific vibrating probe. *J. Cell Biol.* **110:**1565–1573

Lakin-Thomas, P.L., Brody, S., Cote, G.G. 1997. Temperature compensation and membrane composition in *Neurospora crassa*. *Chronobiol. Int.* **14:**445–454

Lampen, J. 1966. Interference by polyenic antifungal antibiotics (especially nystatin and filipin) with specific membrane functions. *In:* Biochemical Studies of antimicrobial drugs. 16th Symposium of Society for General Microbiology. B.A. Newton and P.E. Reynolds, editors. pp. 111–130. Cambridge University Press, London-New York

Lauter, F.R., Yamashiro, C.T., Yanofsky, C. 1997. Light stimulation of conidiation in *Neurospora crassa*: studies with wild type and mutants *wc-1*, *wc-2* and *acon-2*. *J. Photochem. Photobiol.* **37:**203–211

Levina, N.N., Belozerskaya, T.A., Kritsky, M.S., Potapova, T.V. 1988. Photoelectrical responses of *Neurospora crassa* mutant *white collar 1*. *Experiment. Mycol.* **12:**77–79

Levina, N.N., Lew, R.R., Hyde, G.J., Heath, I.B. 1995. The roles of Ca^{2+} and plasma membrane ion channels in hyphal tip growth of *Neurospora crassa*. *J. Cell Sci.* **108:**3405–3417

Lew, R.R. 1989. Calcium activates an electrogenic proton pump in *Neurospora* plasma membrane. *Plant Physiol.* **91:**213–216

Lew, R.R. 1999. Comparative analysis of Ca^{2+} and H^+ flux magnitude and location along growing hyphae of *Saprolegnia ferax* and *Neurospora crassa*. *Eur. J. Cell. Biol.* **78:**892–902

Lewis, B.D., Karlin-Neumann, G., Davis, R.W., Spalding, E.P. 1997. Ca^{2+}-activated anion channels and membrane depolarizations induced by blue light and cold in *Arabidopsis* seedlings. *Plant Physiol.* **114:**1327–1334

Lin, W. 1981. Inhibition of anion transport in corn root protoplast. *Plant Physiol.* **68:**435–438

Lin, C., Robertson, D.E., Ahmad, M., Raibekas, A.A., Jorns, M.S., Dutton, P.L., Cashmore, A.R. 1995. Association of flavin adenine dinucleotide with the *Arabidopsis* blue light receptor CRY1. *Science* **269:**968–970

Linden, H., Ballario, P., Macino, G. 1997. Blue light regulation in *Neurospora crassa*. *Fungal Genet. Biol.* **22:**141–150

Linden, H., Ballario, P., Arpaia, G., Macino, G. 1999. Seeing the light: news in *Neurospora* blue light signal transduction. *Adv. Genet.* **41:**35–54

Long, J.C., Jenkins. 1998. Involvement of plasma membrane redox activity and calcium homeostasis in the UV-B and UV-A/blue light induction of gene expression in *Arabidopsis*. *Plant Cell* **10:**2077–2086

Long, C., Iino, M. 2001. Light-dependent osmoregulation in pea stem protoplasts. Photoreceptors, tissue specificity, ion relationships, and physiological implications. *Plant Physiol.* **125:**1854–69

Lucas, W.J., Kochian, L.V. 1986. Ion transport processess in corn roots: An approach utilizing microelectrode techniques. *In:* Advanced Agricultural Instrumentation: Design and Use. Gensler, W.G., editor. pp. 402–425. Dordrecht: Matinus Nijhoff.

Martinac, B., Buechner, M., Delcour, A.H., Adler, J., Kung, C. 1987. Pressure-sensitive ion channel in *Escherichia coli*. *Proc. Natl. Acad. Sci. USA* **84:**2297–2301

Matty, A., NeherE. 1993. Tight-seal whole-cell recording. *In:* Single Channel Recording. Sakmann, B., Neher, E., editors. pp. 31–52. Plenum Press, New York

Messerli, M.A., Danuser, G, Robinson, K.R. 1999. Pulsatile influxes of H^+, K^+ and Ca^{2+} lag growth pulses of *Lilium longiflorum* pollen tubes. *J. Cell Sci.* **112:**1497–1509

Mitzka, U., Rau, W. 1977. Composition and photoinduced biosynthesis of the carotenoids of a protoplast-like *Neurospora crassa* "slime" mutant. *Arch. Microbiol.* **111:**261–263

Newman, I.A. 2001. Ion transport in roots: measurement of fluxes using ion-selective microelectrodes to characterize transporter function. *Plant Cell Environ.* **24:**1–14

Newman, I.A., Kochian, L.V., Grusak, M.A., Lucas, W.J. 1987. Fluxes of H^+ and K^+ in corn roots. Characterization and stoichiometries using ion-selective microelectrodes. *Plant Physiol.* **84:**1177–1184

Noh, B., Spalding, E.P. 1998. Anion channels and the stimulation of anthocyanin accumulation by blue light in *Arabidopsis* seedlings. *Plant Physiol.* **116:**503–509

Okazaki, Y., Azuma, K., Nishizaki, Y. 2000. A pulse of blue light induces a transient increase in activity of apoplastic K^+ in laminar pulvinus of *Phaseolus vulgaris* L. *Plant Cell Physiol.* **41:**230–233

Parks, B.M., Cho, M.H., Spalding, E.P. 1998. Two genetically separable phases of growth inhibition induced by blue light in *Arabidopsis* seedlings. *Plant Physiol.* **118:**609–615

Potapova, T.V., Levina, N.N., Belozerskaya, T.A., Kritsky, M.S., Chailakhian, L.M. 1984. Investigation of electrophysiological responses of *Neurospora crassa* to blue light. *Arch. Microbiol.* **137:**262–265

Pu, R., Robinson, K.R. 1998. Cytoplasmic calcium gradients and calmodulin in the early development of the fucoid alga *Pelvetia compressa*. *J. Cell Sci.* **111:**3197–3207

Reymond, P., Short, T.W., Briggs, W.R., Poff, K.L. 1992. Light-induced phosphorylation of a membrane protein plays an early role in signal transduction for phototropism in *Arabidopsis thaliana*. *Proc. Natl. Acad. Sci. USA* **89:**4718–4721

Roberts, S.K., Dixon, G.K., Dunbar, S.J., Sanders, D. 1997. Laser ablation of the cell wall and localized patch clamping of the plasma membrane in the filamentous fungus *Aspergillus*: characterization of an anion-selective efflux channel. *New Phytol.* **137:**579–585

Satter, RL., Galston, A.W. 1981. Mechanisms of control of leaf movements. *Annu. Rev. Plant. Physiol.* **32:**83–110

Scarborough, G.A. 1988. Large-scale purification of plasma membrane H^+-ATPase from a cell wall-less mutant of *Neurospora crassa*. *Methods Enzymol.* **157:**574–579

Schlatterer, C., Burakov, S., Zierold, K., Knoll, G. 1994. Calcium-sequestering organelles of *Dictyostelium discoideum:* changes in element content during early development as measured by electron probe X-ray microanalysis. *Cell Calcium* **16:**101–111

Schwerdtfeger C, Linden, H. 2000. Localization and light-dependent phosphorylation of white collar 1 and 2, the two central components of blue light signaling in *Neurospora crassa*. *Eur. J. Biochem.* **267:**414–422

Shabala, S., Babourina, O., Newman, I. 2000. Ion-specific mechanisms of osmoregulation in bean mesophyll cells. *J. Exp. Bot.* **51:**1243–1253

Shabala, S., Newman, I.A. 1999. Light-induced changes in hydrogen, calcium, potassium, and chloride ion fluxes and concentrations from the mesophyll and epidermal tissues of bean leaves. Understanding the ionic basis of light-induced bioelectrogenesis. *Plant Physiol.* **119:**1115–1124

Shabala, S.N., Newman, I.A., Morris, J. 1997. Oscillations in H^+ and Ca^{2+} ion fluxes around the elongation region of corn roots and effects of external pH. *Plant Physiol.* **113:**111–118

Shabala, L., Ross, T., Newman, I., McMeekin, T., Shabala, S. 2001a. Measurements of net ion fluxes and extracellular changes of H^+, Ca^{2+}, K^+ and NH^{4+} in *Eschericia coli* using ion-selective microelectrodes. *J. Microbiol. Methods* **46:**119–129

Shabala, L., Shabala, S., Ross, T., McMeekin, T. 2001b. Membrane transport activity and ultradian ion flux oscillations associated with cell cycle of *Thraustochytrium sp. Austral*. *J. Plant Physiol.* **28:**87–99

Silverman-Gavrila, L.B., Lew, R.R. 2001. Regulation of the tip—high $[Ca^{2+}]$ gradient in growing hyphae of the fungus *Neurospora crassa*: *Eur. J. Cell Biol.* **80:**379–390

Shinkle, J.R., Jones, R.L. 1988. Inhibition of stem elongation in *Cucumis* seedlings by blue light requires calcium. *Plant Physiol.* **86:**960–966

Sineshchekov A.V., Lipson, E.D. 1992. Effect of calcium on dark adaptation in *Phycomyces* phototropism. *Photochem. Photobiol.* **56:**667–765

Slayman, C. 1965. Electrical properties of *Neurospora crassa*. Effects of external cations on the intracellular potential. *J. Gen. Physiol.* **49:**69–92

Spalding, E.P., Cosgrove, D.I. 1992. Mechanism of blue-light induced plasma-membrane depolarization in etiolated cucumber hypocotyls. *Planta* **188:**199–205

Standen, N.B., Stanfield, P.R. 1978. A potential- and time-dependent blockade of inward rectification in frog skeletal muscle fibres by barium and strontium ions. *J. Physiol.* **280:**169–191

Strauss, U., Herbrik, M., Mix, E., Schubert, R., Rolfs, A. 2001. Whole-cell patch-clamp: true perforated or spontaneous conventional recordings? *Pfluegers Arch.* **442:**634–638

Suh, S., Moran, N., Lee, Y. 2000. Blue light activates potassium-efflux channels in flexor cells from *Samanea saman* motor organs via two mechanisms. *Plant Physiol.* **123:**833–843

Talora, C., Franchi, L., Linden, H., Ballario, P., Macino, G. 1999. Role of a white collar-1-white collar-2 complex in blue-light signal transduction. *EMBO J.* **18:**4961–4968

Trevithick, J.R., Galsworthy, P.R. 1977. Morphology of *slime* variants of *Neurospora crassa* growing on a glass surface in liquid medium. 1. Under normal conditions and 2. In the presence of inhibitors. *Arch. Microbiol.* **115:**109–118

Valenzuela, C., Ruiz-Herrera, J. 1989. Inhibition of phototropism in *Phycomyces* sporangiophores by calmodulin antagonist and antimicrotubular agents. *Curr. Microbiol.* **18:**11–14

Van Duijn, B., Ypey, D.L., Van der Molen, L.G. 1988. Electrophysiological properties of *Dictyostelium* derived from membrane potential measurements with microelectrodes. *J. Membrane Biol.* **106:**123–134

Very, A.-A., Davies, J.M. 2000. Hyperpolarization-activated calcium channels at the tip of *Arabidopsis* root hairs. *Proc. Natl. Acad. Sci. USA* **97:**9801–9806

Vogel, H. 1956. A convenient growth medium for *Neurospora*. *Microb. Genet. Bull.* **13:**42–46

Wang, X., Iino, M. 1997. Blue-light-induced shrinking of protoplasts from maize coleoptiles and its relationship to coleoptile growth. *Plant Physiol.* **114:**1009–1020

Wang, X., Iino, M. 1998. Interaction of cryptochrome 1, phytochrome, and ion fluxes in blue light-induced shrinking of *Arabidopsis* hypocotyl protoplasts. *Plant Physiol.* **117:**1265–1279

Watts, H.J., Very, A.A., Perera, T.H., Davies, J.M., Gow, N.A. 1998. Thigmotropism and stretch-activated channels in the pathogenic fungus *Candida albicans*. *Microbiology* **144:**689–695

Weiss, J., Weisenseel, M.H. 1990. Blue light-induced changes in membrane potential and intracellular pH of *Phycomyces* hyphae. *J. Plant Physiol.* **136:**78–85

Zhou, X.-L., Stumpf, M.A., Hoch, H.C., Kung, C. 1991. A mechanosensitive channel in whole cells and in membrane patches of the fungus, *Uromyces*. *Science* **253:**1415